Dynamics of Intumescence of Fire-Retardant Polymeric Materials

VADIM SH. MAMLEEV,[1] ESEN A. BEKTUROV,[1] KONSTANTIN M. GIBOV[2]

[1]A. B. Bekturov Institute of Chemical Sciences, Kazakh Academy of Sciences, Valikhanov str. 106, Kazakhstan, Almaty 480100

[2]Higher Technical Fire-School, Moscow broad str. 149, Russia, St.-Petersburg

Received 7 November 1997; accepted 6 March 1998

ABSTRACT: A new numerical method allowing one to estimate a temperature field in an intumescent fire-retardant coating is proposed. The data on heat conductivity of the material, on kinetics of its decomposition, and on kinetics of change of its rheological properties serve for calculation of input parameters. On the basis of experimental information about curing kinetics, the algorithm computes a viscosity of the material in each elementary layer of the coating. It is assumed that the local change of viscosity, in turn, predetermines a local expansion coefficient of the coating. The results of the calculations are compared with the experimental data obtained for the coating on the basis of phenol–formaldehyde resin and boron oxide. © 1998 John Wiley & Sons, Inc. J Appl Polym Sci 70: 1523–1542, 1998

Key words: fire retardants; cellular polymers; intumescence; foaming; modeling

INTRODUCTION

Despite the obvious practical interest in the creation of intumescent fire-retardant paints and coatings, the development of quantitative theory of the intumescence process progresses very slowly.

As far as we know, there exist only several works[1–6] dedicated to thermophysical models of intumescence (foaming). The most detailed one of them was suggested by Clark and coworkers.[1] Clark has assumed that decomposition of the coating material takes place as a result of two reactions. Only the first one of these reactions causes an intumescence. Thus, a zone of passing of this reaction corresponds to zone of intumescence within the coating. If all gas released in the first reaction were retained in the foam, Clark's model would be reasonable enough. However, in reality, as a rule, only a small part of gas is kept in the foam. Therefore, an extent of foaming is determined rather by viscoelastic properties of the material than by amount of gas isolated.

The work of Anderson and Wauters[2] is practically a reproduction of the model of Clark and seems to be a failure. When describing decomposition of the material, these authors ignored the laws of chemical kinetics. Instead of using the Arrhenius equations, they approximated a curve of decomposition by the Fourier series. In contrast to the model of Clark, according to which, foaming takes place only within some region of the coating, the model of Anderson and Wauters[2] implies that foaming occurs in each coating layer undergoing decomposition up to the surface of the coating. At the same time, it is quite obvious that foaming must cease when the melted (liquid) polymer turns into a solid coke. We suppose[3,4] that probably the end of the

Correspondence to: V. Sh. Mamleev.

Contract grant sponsor: INTAS; contract grant number: INTAS–93–1846.

Journal of Applied Polymer Science, Vol. 70, 1523–1542 (1998)

 CCC 0021-8995/98/081523-20

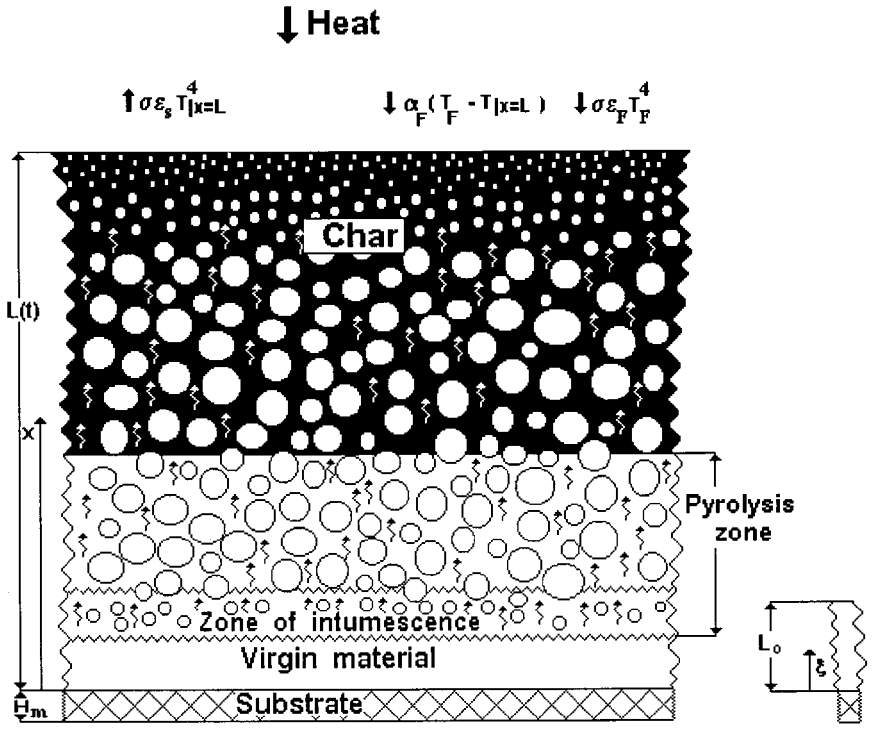

Figure 1 The model of an intumescent coating.

foam formation occurs even earlier, when the material hardens as result of some curing reaction in the polymer.

Buckmaster et al.[5] apparently took into account the inaccuracies of Wauters and made assumptions being, in a sense, opposite to those of Wauters; namely, they assumed that the foaming occurs in the extremely narrow temperature range. This model allows one to explain some peculiarities of dynamics of heating the coatings,[5,6] but being very formal, it by no means reflects the chemical processes of foaming.

It is reasonable to assume[3,4] that in systems with intensive foaming, the reactions of curing and gas formation should be synchronized. Earlier,[3,4] we have offered a numerical procedure calculating the factor of expansion of a coating via an amount of gas held in the foam within a certain range of changing a viscosity of the material. This procedure is illustrated[4] for an artificial example when the heating of a material takes place by the linear law.

The goal of the present article is to consider a model in which local heating of a substance in a coating obeys the heat conduction equation. Such a model allows one to investigate how kinetic parameters of above reactions influence a final behavior of a coating under conditions of actual heating by a flame or other source of heat.

THEORETICAL APPROACH

Equations of Mass Conservation

Foam formation results in the widening of local portions of the substance, that is, in a decrease of density of the material. Current x and initial ξ coordinates of the moving material point (see Fig. 1) are connected by the following equation:

$$x(\xi, t) = \xi + \int_0^t u(\xi, \theta) d\theta$$

where $u(\xi,t)$ is the linear velocity of the movement of the material point. The coordinates x and ξ are the coordinates of Euler and Lagrange, respectively.

The expansion coefficient is connected with the difference of the velocities of two points, being at the initial moment in the positions ξ and $\xi + d\xi$. It is expressed as follows:

$$E(\xi, t) = \partial x / \partial \xi = 1 + \int_0^t [\partial u(\xi, \theta)/\partial \xi] d\theta$$

where

$$\partial u(\xi, t)/\partial \xi = \partial E(\xi, t)/\partial t$$

Let us consider the velocity of the substance flow at a distance x from the back wall (the substrate):

$$dx/dt = v(x, t) \quad (1)$$

It is noteworthy that velocities $u(\xi,t)$ and $v(x,t)$ are not equal, because in eq. (1) it is not determined what portion of the substance at the moment t reaches the x position. However, let us choose a certain portion, fixing its initial coordinate as follows:

$$x_{|t=0} = \xi, \ \partial x/\partial \xi_{|t=0} = 1 \quad (2)$$

Now the velocity value is determined at so-called[7] characteristic $x(\xi,t)$; that is, $v(x,t) = v(x(\xi,t),t) = u(\xi,t)$. Differentiating eq. (1) by ξ leads to the equation

$$d/dt(\partial x/\partial \xi) = \partial v/\partial x(\partial x/\partial \xi) \quad (3)$$

Solving with respect to $\partial x/\partial \xi$ an ordinary differential eq. (3) under the initial condition (2), we obtain

$$E(\xi, t) = \partial x/\partial \xi = \exp\{\int_0^t [\partial v(x(\xi, \theta), \theta)/\partial x]d\theta\} \quad (4)$$

One can readily see that by means of the simple transformations, eq. (4) turns into an identity, as follows:

$$E = \exp[\int_0^t \partial v/\partial \xi(\partial \xi/\partial x)d\theta] = \exp[\int_0^t (\partial \ln E/\partial \theta)d\theta] \equiv E$$

To calculate the change of a local density of the coating we have to do a number of assumptions. First, we shall neglect a temperature coefficient of expansion of polymer mass of the coating. Second, we shall neglect the movement of the mass of the material connected with gravity.

Third, we shall consider that only gases isolated in each elementary layer of the coating take part in the foam formation inside this layer. As to the gases isolated in the lower layers, these penetrate freely through the layer under consideration toward the surface of the coating.

Fourth, we shall assume that all the gas in the coating is under atmospheric pressure P. The latter assumption is required to not include a correction for an excess pressure in bubbles when using the equation of Clapeyron–Mendeleev. This approximation needs to be explained.

An Laplacian excess pressure is essential in bubbles of a size ~ 1 μm. At the same time, gas in the foam is accumulated mainly in bubbles of a size $\sim$ 0.01–1 mm. Therefore, the Laplacian component of the excess pressure can be neglected at once. A reactive component of the excess pressure connected with plastic deformation of a material in the course of growth of bubbles is small while the material remains liquid, but it can sharply rise after gelation (solidification) of the polymer. It was shown[4] that the foam formation begins to occur at a viscosity $\sim$ 300 Pa $\times$ s. At a viscosity $\sim$ 3000 Pa $\times$ s, the material is still able to viscous flow. However, the moment of time of gelation practically coincides with the moment of reaching the viscosity $\sim$ 3000 Pa $\times$ s; that is, an amount of gas that is retained in the foam when changing a viscosity from 300 to 3000 Pa $\times$ s is much greater than that being held in the foam when changing a viscosity from 3000 Pa $\times$ s to ∞. In other words, the gas bubbles, which cross over a very narrow zone of gelation, harden, having no time to grow. After gelation, the excess pressure can lead to a rupture of bubbles' walls, but since the material is a solid one, the hardened bubbles conserve their volume and form (merely closed hollows turn into open ones). We note that the latter fact is confirmed by investigation of slits of the coatings. Thus, when calculating a change of the expansion coefficient, one may ignore a correction for the excess pressure in the equation of Clapeyron–Mendeleev up to the moment of gelation and consider that the expansion coefficient reaches a limit (stationary) value after the moment of gelation.

With the assumption made in the chosen layer of the coating (see Fig. 2), a density decreases due to the foam formation and due to decrease in the layer mass resulting from chemical decomposition of the material.

Depending on a position of a layer under consideration, gases isolated upon decomposition can leave this layer either due to disintegration of

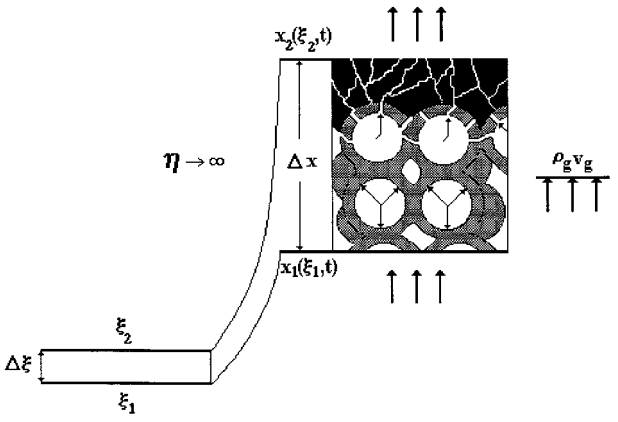

Figure 2 The evolution of a small fragment of a coating.

bubbles (the region of a liquid foam) or due to filtration through the system of micropores in the solid material (the region of a solid foam).

To apply the laws of formal kinetics, one should consider the gas isolation as being a result of decomposition of several individual components. Let us consider first, for the sake of simplicity, a case of one-component media. If the component undergoes chemical decomposition, the continuity equation in Euler and Lagrange coordinates has the following form:

$$\partial\rho/\partial t + \partial\rho v/\partial x = -d\Gamma/dt \tag{5}$$

$$d\rho/dt + \rho\partial v/\partial x = -d\Gamma/dt \tag{6}$$

where ρ is a density of the component, and $-d\Gamma/dt$ is a source of a loss of mass due to the decomposition reaction. If the component does not decompose, then $d\Gamma/dt = 0$. The function Γ depends both upon x (or ξ) and upon t; however, partial derivative of Γ with respect to x (or ξ) will be nowhere used below, and so in an expression for Γ, the x (or ξ) variable can be considered as a parameter. That is why in eqs. (5) and (6), we used full derivative of Γ with respect to time.

In eq. (6), we used the known[7] designation

$$d\rho/dt = \partial\rho/\partial t_{|\xi=\text{const}} = \partial\rho/\partial t_{|x=\text{const}} + v\partial\rho/\partial x$$

Indeed, if the functions $\partial v/\partial x$ and $d\Gamma/dt$ are formally considered as known ones, eq. (6) becomes an ordinary differential equation with respect to ρ, in which ξ is some parameter and is not an independent variable.

To determine a form of the function $d\Gamma/dt$, let us consider the change of mass of the component Δm within a segment between two characteristics (see Fig. 2)

$$d\Delta m/dt = Ad/dt \int_{x_1(\xi_1,t)}^{x_2(\xi_2,t)} \rho dx = A\,(\rho v_{|x=x_2} - \rho v_{|x=x_1} + \int_{x_1(\xi_1,t)}^{x_2(\xi_2,t)} (\partial\rho/\partial t)dx)$$

where A is the surface area under consideration that is perpendicular to the flow.

Using eq. (5), it is easy to show that

$$d\Delta m/dt = -A \int_{x_1}^{x_2} (d\Gamma/dt)dx \tag{7}$$

The function $\Delta m/\Delta m_0$, where Δm_0 is the initial mass of the component, conforms to the laws of formal kinetics. It is noteworthy that this mass ratio does not depend on absolute values of the masses; that is, $\Delta m/\Delta m_0 = m/m_0$. The function $m(t)/m_0$ (the curve of the mass loss) is usually measured by means of thermogravimetric analysis. It can be expressed generally by the following differential equation:

$$d\,(m/m_0)/dt = -k_c(m/m_0)^n \exp(-E_c/RT)$$

where E_c is an activation energy, T is temperature, k_c is a rate constant, n is an order of reaction, and R is the gas constant.

Integration gives

$$m/m_0 = f(\tau) = [k_c\tau(n-1)+1]^{-1/(n-1)},\ (n > 1)$$

$$m/m_0 = f(\tau) = \exp(-k_c\tau),\ (n = 1)$$

where

$$\tau[T(\theta)]_{|\theta=t} = \int_0^t \exp[-E_c/RT(\theta)]d\theta \tag{8}$$

is the reduced reaction time.

We put the double brackets in the left-hand side of eq. (8), assuming that τ is a functional and not a function of temperature. Further, we shall use the expression $\tau = \tau(t)$, for brevity, bearing in

mind, however, that $\tau(t)$ is unambiguous function of time only with a fixed temperature–time dependence $T(t)$.

Note that $\Delta m_0 = A\rho_0\Delta\xi$, where ρ_0 is the initial density of the component. Thus, from eq. (7), we obtain

$$\rho_0\Delta\xi df/dt \approx -\Delta x d\Gamma/dt$$

Going to the limit at $\Delta\xi \to 0$ ($\Delta x \to 0$), we have

$$d\Gamma/dt = -[\rho_0/E(\xi, t)]df/dt \tag{9}$$

Substituting expression (9) into eq. (6) and integrating with respect to $\rho(\xi,t)$ the ordinary differential equation (6) under the initial condition $\rho(\xi,0) = \rho_0(\xi) = \rho_0$, we obtain

$$\rho(\xi, t) = \rho_0\exp(-I)\{1 + \int_0^t [\exp(I)/E(\xi, \theta)] \times (df/d\theta)d\theta\}$$

where

$$I = \int_0^t [\partial v(x(\xi, \theta), \theta)/\partial x]d\theta$$

Taking into account eq. (4), one can readily see that

$$\rho(\xi, t) = [\rho_0/E(\xi, t)]f(\tau)$$

The latter equation may be deduced from eqs. (6) and (7) by one more manner,

$$E[d\rho/dt + \rho\partial v/\partial\xi(\partial\xi/\partial x)] = Ed\rho/dt + \rho\partial E/\partial t = d(E\rho)/dt = d(\rho_0 f)/dt$$

From here, $E\rho = \rho_0 f$.

For going to the case of a media consisting of N components, it is sufficient to use the rule of additivity to give

$$\rho(\xi, t) = \sum_{i=1}^{N} \rho_i(\xi, t) = [\rho_0/E(\xi, t)] \sum_{i=1}^{N} w_i f_i(\tau_i)$$

$$d\Gamma/dt = -[\rho_0/E(\xi, t)] \sum_{i=1}^{N} w_i df_i(\tau_i)/dt \tag{10}$$

where $w_i = \rho_{o,i}/\rho_0$ ($1 \le i \le N$) are mass fractions of the components. Being calculated per gram of the coating, the mass of gaseous products q isolated to the moment t at the point with the initial coordinate ξ constitutes

$$q(\xi, t) = \sum_{i=1}^{N} w_i[1 - f_i(\tau_i)] = 1 - \sum_{i=1}^{N} w_i f_i(\tau_i)$$

The volume of this mass is equal to $RT(\xi,t)q/PM$, where M is the molecular weight of the gas.

Thermogravimetric dependence (the curve of the mass loss) for multicomponent system is expressed as

$$m[T(\theta)]_{|\theta=t}/m_0 = \sum_{i=1}^{N} w_i f_i(\tau_i[T(\theta)]_{|\theta=t})$$

The algorithm of the $E(\xi,t)$ calculation, proposed earlier,[3,4] is based on the hypothesis that the gas released is retained in the foam only in a certain range of rheological state of the material when its dynamic viscosity varies within the limits $[\eta_m,\infty)$. At the point of coating with the initial coordinate ξ, the time interval $[t_{\min}(\xi), t_{\max}(\xi)]$ corresponds to the viscosity interval $[\eta_m,\infty)$. Thus, a gas volume kept in the foam is equal to

$$(RT/PM)\tilde{q}(\xi, t) = \begin{cases} 0, & t < t(\eta_m(\xi)) = t_{\min}(\xi) \\ (RT/PM)[q(\xi, t) - q(\xi, t_{\min})], & t_{\min} < t < t_{\max} \\ (RT(\xi, t_{\max})/PM)q_{\max}, & t > t(\eta(\xi) \to \infty) = t_{\max}(\xi) \end{cases} \tag{11}$$

Initially, a gram of the coating occupies a volume of $1/\rho_0$. Due to the decomposition of the material, this volume decreases. If we assume that the decrease in the volume is proportional to the lost mass, then the volume of polymer mass under consideration will constitute $(1 - q)/\rho_0$. The overall volume of the foam is a sum of the volume of polymer mass and the volume of isolated gas.

Hence, the ratio of the volume of the foam to the initial volume of the coating is equal to

$$E(\xi, t) = [(1 - q)/\rho_0 + \tilde{q}(\xi, t)RT(\xi, t)/PM]/(1/\rho_0)$$

$$= 1 - q + \rho_0\tilde{q}(\xi, t)RT(\xi, t)/PM,$$

$$t_{\min}(\xi) < t < t_{\max}(\xi) \quad (12)$$

If presuming that the sole result of the material gasification is the increase in porosity, it is easy to express the volume fractions of the retained gas ω_g and the polymer mass ω_p as follows:

$$\omega_g = (E - 1 + q)/E, \ \omega_p = (1 - q)/E \quad (13)$$

The actual density of the material is equal to

$$\rho = \omega_p\rho_0 + \omega_g\rho_g \quad (14)$$

where ρ_g is the gas density. Formulas (10) and (14) differ because eq. (10) describes the change of a partial density. However, since $\rho_0 \gg \rho_g$, equations (10) and (14) give close results.

Let us derive the equation of a material balance for the gaseous phase, considering again the layer between 2 characteristics (see Fig. 2). Taking account of eq. (7), one can write

$$\rho_g v_{g|x=x_2} - \rho_g v_{g|x=x_1} = \int_{x_1}^{x_2} (d\Gamma/dt)dx - d/dt \int_{x_1}^{x_2} \omega_g\rho_g dx \quad (15)$$

where v_g is the velocity of gas movement. When substituting the expression for ω_g from eq. (13) into eq. (15) and using integration along Lagrange coordinate, we obtain

$$\rho_g v_{g|x=x_2} - \rho_g v_{g|x=x_1} = \rho_0 \int_{\xi_1}^{\xi_2} (dq/dt)d\xi - d/dt \int_{\xi_1}^{\xi_2} E\rho_g d\xi + d/dt \int_{\xi_1}^{\xi_2} (1 - q)\rho_g d\xi \quad (16)$$

While the foaming takes place, the equality $dq/dt = d\tilde{q}/dt$ should be fulfilled. Using eqs. (11) and (12) for the stage of foam formation from eq. (16), we find

$$\rho_g v_{g|x=x_2} - \rho_g v_{g|x=x_1 = 0}$$

In other words, at this stage, all the gas isolated within the layer under consideration is retained in the foam. Note that the latter result is a natural consequence of our initial assumption.

At the limit $\Delta\xi \to 0$, eq. (16) gives

$$\partial\rho_g v_g/\partial\xi + d(E - 1 + q)\rho_g/dt = \rho_0 dq/dt \quad (17)$$

We used, in eq. (17), the full derivatives with respect to time, just like in eq. (6), keeping in mind that all the functions in this equation are given in Lagrange coordinate system. We note that eq. (17) describes the balance of gas within layers that move with the velocity of the polymer substance. However, a velocity of gas differ from a velocity of polymer ($v_g \neq v$); therefore, eq. (17) is not the continuity equation for gas.

By expressing the gas density as $\rho_g = PM/RT$, one may rewrite eq. (17) as follows:

$$\partial\rho_g v_g/\partial\xi = \rho_0 dq/dt - \rho_g d(E + q)/dt + (PM/RT^2)(E - 1 + q)dT/dt \quad (18)$$

The second and third terms in the right-hand part of eq. (18) correspond respectively to the retention of gas in the material due to foaming and to the gas flow connected with thermal expansion of gas in pores. Since the retention of gas in the foam usually is much less than the amount released on the whole, these terms can be omitted. Taking into account that the gas flow at the back wall is equal to zero, one can write with good accuracy the gas flow as

$$\rho_g v_{g|x=x(\xi,t)} = \rho_0 \int_0^{\xi} (dq/dt)d\xi \quad (19)$$

Cagliostro et al.[1] used eq. (19) in their calculations, although a more accurate equation has the following form:

$$\rho_g v_{g|x=x(\xi,t)} = \int_0^{\xi} G(\xi, t)d\xi$$

where

$$G(\xi, t) = \begin{cases} 0, & t_{\min} < t < t_{\max} \\ \rho_0 dq/dt - d(E - 1 + q)\rho_g/dt, & t < t_{\min},\ t > t_{\max} \end{cases}$$

Equation of Energy Conservation

Equation of heat conduction in the Euler coordinate system is as follows:

$$(c_g\rho_g\omega_g + c_p\rho_p\omega_p)\partial T/\partial t + [c_g\rho_g v_g + v(c_g\rho_g\omega_g + c_p\rho_p\omega_p)]\partial T/\partial x + (\rho_0/E)\sum_{i-1}^{N}\Delta H_i w_i df_i(\tau_i)/dt = \partial/\partial x(\lambda\partial T/\partial x)$$

where c_g and c_p are the specific heat capacities of the gas and polymer mass, ΔH_i $(1 \le i \le N)$ are heat effects of decomposition reactions of the components, and λ is the heat conductivity. By taking account of the equality

$$\partial T/\partial t_{|\xi=\text{const}} = \partial T/\partial t_{|x=\text{const}} + v\partial T/\partial x$$

let us go into the Lagrange coordinates

$$E(c_g\rho_g\omega_g + c_p\rho_p\omega_p)\partial T/\partial t + c_g\rho_g v_g\partial T/\partial\xi + \rho_0\sum_{i=1}^{N}\Delta H_i w_i df_i(\tau_i)/dt = \partial/\partial\xi[(\lambda/E)\partial T/\partial\xi] \quad (20)$$

The first term in the left-hand part of eq. (20) takes into account the accumulation of heat in the coating; the second term takes into account the convective transfer by the decomposition gases; the third term takes into account the heat effect of the decomposition reactions; finally, the right-hand part corresponds to the heat exchange through the material of the coating.

If neglecting the accumulation of heat by gases being in the pores $c_g\rho_g\omega_g \ll c_p\rho_p\omega_p$ and taking into account the equality $\omega_p E = 1 - q$, the left-hand part of eq. (20) becomes independent of E. Thus, the effect of the retardancy of heating caused by intumescence can be explained[1] exclusively in terms of an effective heat conductivity: $\lambda_{\text{effective}} = \lambda/E$.

The value λ, according to the studies of Anderson et al.,[8] is approximated satisfactory as

$$\lambda = \lambda_g\lambda_p/(\omega_g\lambda_p + \omega_p\lambda_g) = \lambda_g\lambda_p E/[(E - 1 + q)\lambda_p + (1 - q)\lambda_g] \quad (21)$$

where λ_g and λ_p are heat conductivities of gas and polymer mass, respectively.

Since $\lambda_p \gg \lambda_g$, even at low values of E ($E \sim 1.5 - 2$), the local conductivity of the coating is practically stipulated by heat conductivity of gaseous products in the pores. When $E \gg 1$, the veritable heat conductivity λ, in accordance with formula (21), is limited by the heat conductivity of gas ($\lambda \approx \lambda_g$); consequently, the effect of deceleration of heat transfer in the coating is stipulated only by a local expansion, $\lambda_{\text{effective}} = \lambda_g/E$. If, furthermore, the coefficient E has approximately a constant value along the depth of the coating, then the heat-shielding effect is determined solely by the factor of increasing a thickness of the coating.

We note that eq. (21) seems to us to be an imperfect one. In the systems with large pores, the heat conductivity, in particular, should certainly depend on the size of pores.

To solve eq. (20), it is necessary to set boundary conditions as follows:

$$(\lambda/E)\partial T/\partial\xi_{|\xi=L_0} = \alpha_F[T_F - T_{|\xi=L_0}] + \varepsilon_F\sigma T_F^4 - \varepsilon + \varepsilon_F\sigma T^4_{|\xi=L_0} \quad (22)$$

$$(\lambda/E)\partial T/\partial\xi_{|\xi=0} = c_m\rho_m H_m dT/dt_{|\xi=0} + \alpha_B[T_{|\xi=0} - T_0] \quad (23)$$

and initial condition

$$T = T_0,\ \rho = \rho_0,\ t = 0 \quad (24)$$

where T_0 is an initial temperature; T_F is the flame temperature; α_F is the coefficient of heat exchange between flame and coating surface; ε_F and ε_S are the coefficients of emission of the flame and the coating surface; σ is the Stephan–Boltzmann constant; L_0 is the initial thickness of the coating; c_m, ρ_m, H_m are heat capacity, density, and thickness of the substrate; and α_B is the coefficient of heat exchange between the substrate and outer media.

Equations (20)–(24) form the complete system to study numerically the dynamics of intumescent coating.

EXPERIMENTAL

The intumescent coating was prepared[3] at 120°C by mixing 80% by weight of phenol–formaldehyde

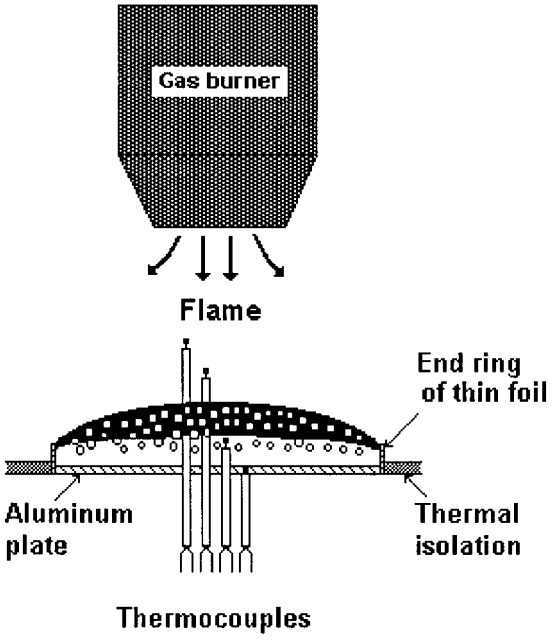

Figure 3 The scheme of testing the coating.

resin (PhFR) and 20% by weight of boron oxide (B_2O_3). Thermogravimetric analysis of this blend was fulfilled by derivatograph MOM (Hungary) in the nitrogen atmosphere at the heating rate of $\approx$ 20°C/min.

A composition layer of 1 cm thickness was put on an aluminum disk with the diameter of 15 cm and thickness of 0.3 cm. A propane air flame, which was created by a gas injector situated at a distance of 10 cm from the initial position of the coating surface (see Fig. 3), served as a source of heat.

The measurements of a temperature were done by chromel–alumel thermocouples with the junction diameter of 200 μm. For avoidance of destruction of the thermocouples' material, the surface of the thermocouples was covered by a film of silicon oxide. The temperature equilibrium between thermocouple and the flame is reached for $\sim$ 10–20 s. This time is much less than that of the experiment.

The thermocouples were fastened at different heights from the back wall (the substrate). A current position of the coating surface relatively to the back wall was measured by a cathetometer.

Initially, the thermocouples are located within the flame and consequently show the flame temperature ($\approx$ 1150°C), but, as the coating foams, the thermocouples penetrate in the depth of the material and, in so doing, display the temperature change in the interior layers of the coating in the Euler coordinate system.

Temperature on the coating surface was measured by optical pyrometer. For $\approx$ 5 min, it reaches the stationary value, which is approximately equal for different regions of the surface and constitutes $\approx$ 850–870°C.

RESULTS AND DISCUSSION

Analysis of Thermogravimetric Data

Kinetic analysis of decomposition of organic polymers by the data of the mass loss is a complicated problem since destruction of polymers is usually characterized by many conjugated reactions. An assumption of independence of these reactions is rather rough, although for practical calculations, it is difficult to choose more rational approximation.

Let us assume that the loss in the mass of the material takes place due to one reaction only. Then the aim of the analysis is the calculation of three constants, as follows: n, k_c, and E_c, by using the mass loss curve. Their calculation is possible by way of the best matching of the theoretical and experimental curves of mass loss in the scale of the logarithm of the reduced time.

Let the temperature value be set in M points $T_j = T(t_j)$, $1 \le j \le M$. In the same points the values of f_j, $1 \le j \le M$ of mass loss are known.

Let us introduce the array $\{y_j\}$, connected with the reduced time of a reaction of nth order as

$$y_j = k_c \tau_j = [(1/f_j)^{n-1} - 1]/(n - 1),\ 1 \le j \le M \tag{25}$$

With high accuracy, the theoretical values of the reduced time are presented as the following finite sum:

$$\tilde{\tau}_j = \int_0^{t_j} \exp[-E_c/RT(\theta)]d\theta \approx \sum_{i=1}^{j-1} \{R\bar{T}_i^2(t_{i+1} - t_i)/$$

$$[E_c(T_{i+1} - T_i)]\}[\exp(-E_cT_i/R\bar{T}_i^2)$$

$$- \exp(-E_cT_{i+1}/R\bar{T}_i^2)] \tag{26}$$

where $\bar{T}_i = (T_{i+1} + T_i)/2$. Upon the preset n, the values of k_c and E_c can be found by minimizing the function

$$\Delta = M^{-1} \sum_{j=1}^{M} (\ln k_c + \ln \bar{\tau}_j - \ln y_j)^2$$

An optimum value of lnk_c is calculated analytically

$$\ln k_c = M^{-1} \sum_{i=1}^{M} \ln(y_i/\bar{\tau}_i) \tag{27}$$

With fixed n, the function

$$\Delta = M^{-1} \sum_{j=1}^{M} [M^{-1} \sum_{i=1}^{M} \ln(y_i/\bar{\tau}_i) - \ln(y_j/\bar{\tau}_j)]^2 \tag{28}$$

depends only on the activation energy E_c. The calculation of the set $\{y_j\}$ by eq. (25) is carried out once. Then, by calculating the set $\{\tau_j\}$ with different E_c by eq. (26), it is possible to find E_c by minimizing the function (28). Thereupon lnk_c is found by eq. (27). Conducting this procedure repeatedly with different n, it is possible to find a minimum of Δ with respect to n, that is, to estimate the reaction order. In the given algorithm, only one-dimensional minimizing of function (28) must be done numerically; that is why the algorithm is simple and reliable.

For calculating the constants in a multicomponent system, it is important that the decomposition stages of different components were separated well. In Figure 4, the thermogravimetric analysis (TGA) results for the blends of 80% PhFR + 20% B_2O_3 and 80% PhFR + 20% H_3BO_3 are shown. It is seen that the decomposition mechanisms of these blends significantly differ. It is noteworthy that rheological characteristics of these compositions also differ very much. In particular, the coating with the addition of boric acid is not able to foam at all.

Decomposition of the blend PhFR with H_3BO_3 has two distinct stages; their contributions constitute $w_1 = 0.175$ and $w_2 = 0.2$. The first stage seems to be connected with the partial destruction of the polymer and isolation of water as a result of the polycondensation reaction, and the second stage is connected with the carbonization of the material. Having carried out the optimizing procedure for each stage, one can find $E_c^{(1)} = 13.46$ kcal/mol, $k_c^{(1)} = 0.96 \times 10^5$ s^{-1}, $n^{(1)} = 2.2$, $E_c^{(2)} = 28.6$ kcal/mol, $k_c^{(2)} = 0.2 \times 10^6$ s^{-1}, and $n^{(2)} = 1$.

In the case of B_2O_3, the stages of the process are separated poorly. Nothing remains, only to suppose that the stage of carbonization has the same characteristics as in the case of H_3BO_3. Then the first stage can be distinguished by difference between the overall curve of decomposition and the mass loss in the reaction of carbonization. The contribution of the first stage constitutes $w_1 = 0.13$. After the optimization, one may obtain the following estimations: $E_c^{(1)} = 5.89$ kcal/mol, $k_c^{(1)} = 0.53$ s^{-1}, and $n^{(1)} = 2.2$.

It is seen from Figure 4 that the theoretical curves calculated by the found constants correspond well to the experimental ones.

Estimation of Heat Conductivity

The coefficient λ is one of main parameters in the coating model; however, its *a priori* estimations are very complicated since these include many individual peculiarities of the coating. That is why it is reasonable to estimate λ on the basis of experimental measurements of the temperature field in the coating (see Fig. 5). When $t \to \infty$, the temperature distribution in the coating reaches the stationary limit $T^{\infty}(x)$ (see Fig. 6). With an increase of time, the rate of destructive processes is decreasing, and the corresponding terms in the heat transfer equation may be omitted. Besides, we can assume, as a first approximation, that the intumescent material possesses constant physical characteristics along the depth. Then, upon a large amount of time, the change of the temperature in the coating will be described by the following system of equations:

$$\partial T/\partial t = \kappa \partial^2 T/\partial x^2 \tag{29}$$

$$T(L_\infty, t) = T_s$$

$$\lambda \partial T/\partial x_{|x=0} = c_m \rho_m H_m dT/dt_{|x=0} + \alpha_B (T_{|x=0} - T_0)$$

$$T(x, t_0) = \varphi(x)$$

where $\kappa = \lambda/c_p\rho$ is a coefficient of temperature conduction, L_∞ is the limited height of the coating, and $\phi(x)$ is the temperature distribution at the moment t_o. Equation (29) probably holds true with good accuracy if the time moment t_o is chosen to be big enough.

It is known from the heat transfer theory[9] that upon a large amount of time, a regular regime of the material heating is reached when the solution

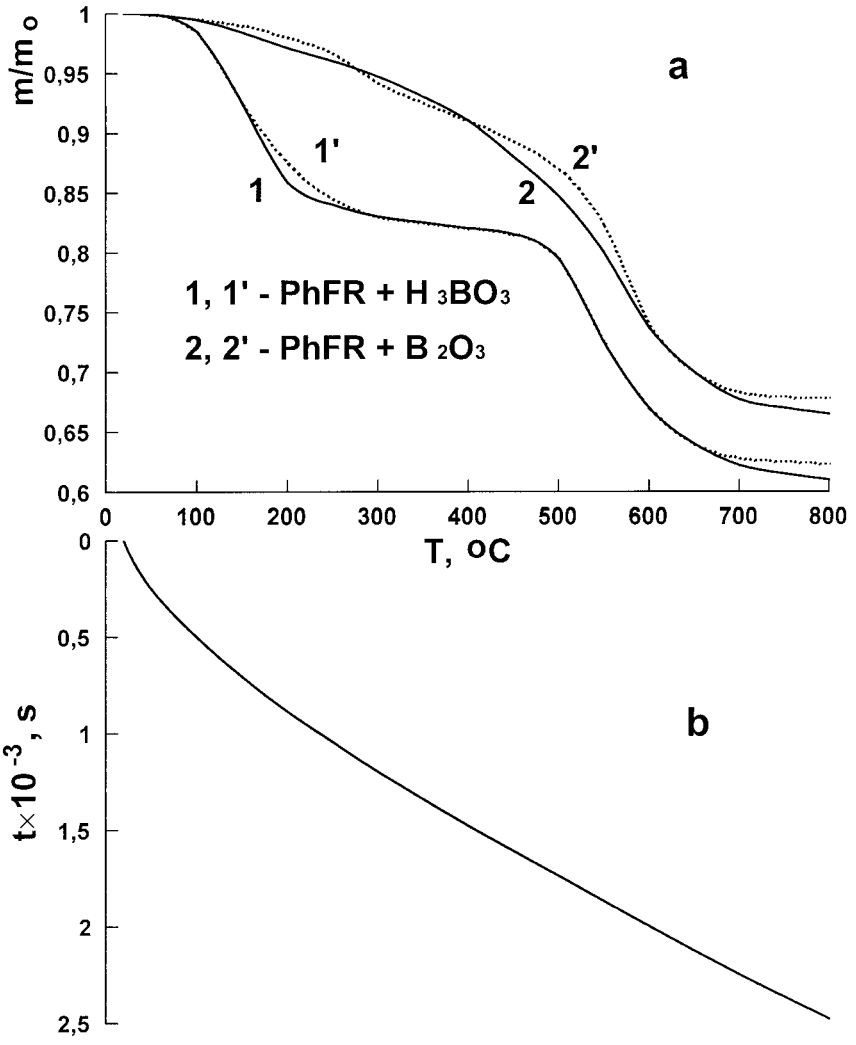

Figure 4 (a) The curves of the mass loss for the blends: (1, 1′) H_3BO_3 + PhFR and (2, 2′) B_2O_3 + PhFR. The experimental (1, 2) and calculated (1′, 2′) results are shown by the solid and dotted lines respectively. (b) The dependence of temperature in a chamber of derivatograph upon time.

of eq. (29) conforms to the exponential dependence, as follows:

$$T(x, t) - T^{\infty}(x) \cong A(x)\exp(-z^2\kappa t/L_{\infty}^2)$$

where $A(x)$ is some function that depends on the coordinate only, and z is a least root of the following equation:

$$ctg(z) = [(c_m\rho_m H_m/\lambda L_{\infty})z^2\kappa - (\alpha_B L_{\infty}/\lambda)]/z \quad (30)$$

The coefficients α_B and λ are connected by the equation

$$\lambda = \alpha_B L_{\infty}(T_B - T_0)/(T_s - T_B) \quad (31)$$

where T_B is the stationary temperature on the back wall. Treatment of the asymptotic intervals of the temperature–time dependencies for upper thermocouples gives the estimation $z^2\kappa/L_{\infty}^2 = 2.3 \times 10^{-3}\ s^{-1}$. A number of parameters, which are included in eqs. (30) and (31), can be estimated as $c_m\rho_m H_m = 0.175$ cal/cm × °C, $c_p = 0.4$ cal/g × °C, $\rho_0 = 1.13$ g/cm^3, $\rho = \rho_0(1 - w_1 - w_2)\ L_0/L_{\infty} = 0.15$ g/cm^3, $L_0 = 1$ cm, $L_{\infty} = 4.6$ cm, and $T_B = 200$°C. Thus, eqs. (30) and (31) contain only two unknown parameters, α_B and λ. Solving the system of two equations, we find

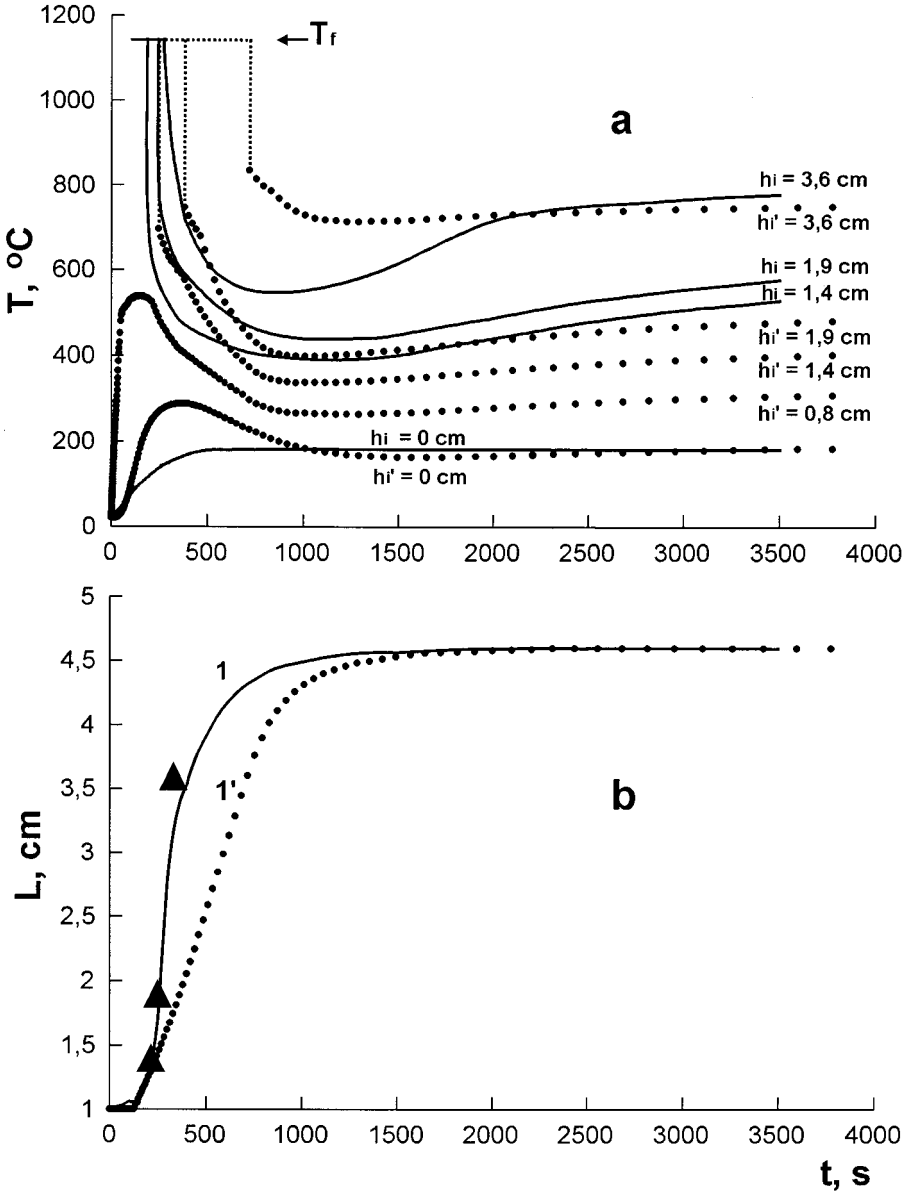

Figure 5 (a) The indications of the thermocouples fastened at different heights (in cm) from the back wall. The experimental (h_i) and numerically calculated (h_i') results are shown by the solid lines and by points, respectively. The dotted lines display a discontinuity between the flame temperature and a temperature on a surface of the coating. (b) The experimental (1) and calculated (1′) dependencies of the height of the coating upon time. The points resulted from the indications of the thermocouples at moments of their crossing with surface of the coating.

$\alpha_B = 4.9 \times 10^{-4}$ cal/cm^2 × s × °C and $\lambda = 8.6 \times 10^{-4}$ cal/cm × s × °C.

It follows from Figure 6 that the heat conductivity, in fact, depends on the coordinate. Considering α_B as a known parameter and coming from the condition

$$\lambda \partial T/\partial x_{|x=0,t\to\infty} = \alpha_B(T_B - T_0)$$

we can define more accurately the λ value on the back wall, as follows: $\lambda = 5.5 \times 10^{-4}$ cal/cm × s × °C. The λ value on the surface of the coating is approximately thrice greater and equal to 1.8×10^{-3} cal/cm × s × °C. This fact can be explained by that the carbonized material has higher heat conductivity than the noncarbonized polymer. Heat conductivity of coke[8] is equal to 5.4×10^{-2}

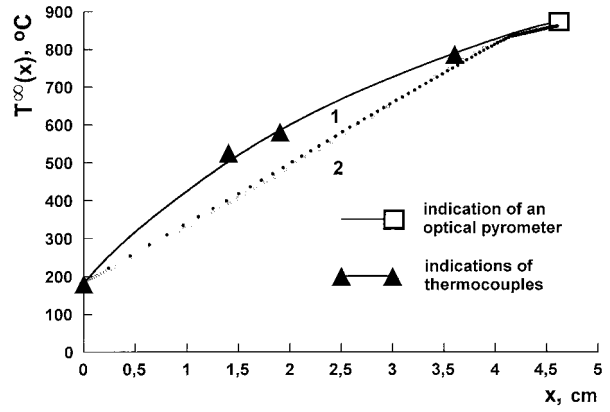

Figure 6 The stationary distribution of temperature along a depth of the coating (1) according to the model implying the critical threshold of viscosity η_m, and (2) according to the model of foam draining. The indications of thermocouples corresponds to Figure 5.

cal/cm × s × °C, and that of the polymer[1] is about 10^{-3} cal/cm × s × °C. If we take such values then, according to eq. (21), the heat conductivity of gas is $\lambda_g = 5.1 \times 10^{-4}$ cal/cm × s × °C. With such a parameter, eq. (21) describes well the boundary values of λ, although all the coefficients obtained are effective. In particular, besides heterogeneity of the material along depth, the calculated values can be affected also by non-one-dimensional geometry of the coating due to the limited diameter of the back wall.

Calculation of the Temperature Field in the Coating

The system of eqs. (20)–(24) was solved by an explicit method of finite difference with 101 equidistant knots on a coordinate grid. We envisaged a calculation scheme of the second order of approximation by coordinate and the first one by time. According to the standard method,[10] the solution is found at the following knot points: $T_{ij} = T(\xi_i,t_j)$, $\xi_i = (i - 1)L_0/(I - 1)$, $i = 1,2, \ldots, I$; $t_j = t_{j-1} + \Delta t_j$, and $j = 1,2, \ldots,$ where I is the number of spatial knots ($I = 101$), and Δt_j is a time step.

Since the system is essentially nonlinear, it is necessary to carry out iterations at each time step. As a feature of convergence of the iterations, the following criterion was used:

$$\sum_{i=1}^{I} |1 - T_{ij}^{(p+1)}/T_{ij}^{(p)}| < 10^{-4}$$

where 1 is an iteration counter. The practice of calculations has shown that upon simple iterations, the convergence by given criterion often is not reached. However, the convergence was always attained when a scheme with relaxation was used for the calculation of the corrected values of temperature, heat conductivity, and expansion coefficient, namely,

$$T_{ij} = (T_{ij}^{(p)} + T_{ij}^{(p+1)})/2$$

$$\lambda_{ij} = (\lambda_{ij}^{(p)} + \lambda_{ij}^{(p+1)})/2$$

$$E_{ij} = (E_{ij}^{(p)} + E_{ij}^{(p+1)})/2$$

An algorithm of the calculation of expansion coefficient was described earlier.[3,4] A peculiarity of the thermophysical problem is that the value $E(\xi,t)$ should be calculated at each layer of the coating and at each time step. The sequence of the calculations is as follows. First, at each knot point, a composition viscosity is calculated. If its value is within the interval $[\eta_m, \infty)$, the values of t_{min} and t_{max} corresponding to the limits of the stable foam formation are calculated by solving with respect to t the transcendental equations of the form $\eta(\xi,t) = \eta_m$ and $\eta(\xi,t) \to \infty$. When calculating t_{min} and t_{max}, the assumption of the linearity in the change of temperature with time in each layer of the coating within the limits of a time step was used.

Earlier[3,4] we noted that at a high temperature, the process of carbonization seemed to suppress foaming. This circumstance was taken into account in the following way. If the value of t_{min} in the certain layer of the coating corresponded to the temperature > 500°C, that layer was considered unable to foam up. If the value of t_{max} corresponded to the temperature > 500°C, the value of t_{max} was assumed to be equal to a time moment necessary for heating the given layer to 500°C. Thus, carbonization completely or partially suppressed foaming.

After determination of the knot values of the expansion coefficient E_{ij} it is easy to calculate density of the coating by eqs. (13) and (14) and heat conductivity by eq. (21). Depending on the temperature value in a layer, either the heat conductivity of the initial polymer (if $T_{ij} < 500$°C) or the heat conductivity of coke (if $T_{ij} > 500$°C) was substituted in eq. (21) as λ_p.

To calculate the indications of the immovable thermocouples, it is necessary to recalculate the Lagrange coordinates into the Euler system.

This transition was accomplished by calculation of the knot points in the Euler system and liner interpolation of the temperature between the points. The grid chosen was dense enough; that is why interpolation yielded high accuracy.

The parameters of the curing reaction, used in calculations, were given earlier.[3,4] Apart from thermophysical parameters described in previous sections, the values obtained by the other authors were used.[1,2] The heat effect of the first decomposition reaction ΔH_1 was assumed to be equal to zero. The heat effect of carbonization ΔH_2 was assumed[1] to be -2000 cal/g. Besides, the following parameters[2] of heat exchange were used: $\varepsilon_F = 1$, $\varepsilon_s = 1$, $\alpha_F = 3 \times 10^{-4}$ cal/cm$^2 \times s \times$ °C, and $c_g = 0.15$ cal/g $\times$ °C.

Only the parameter η_m was varied by comparing of the model with the experiment. The value of η_m determines the region of foam formation and, correspondingly, the maximum expansion coefficient $E_f(\xi) = E(\xi, t_{max}(\xi))$. Concrete distribution of the maximum expansion coefficient by a coordinate determines, in turn, the final height of the coating. The value of η_m was varied in the calculation so as to obtain the following observed final height of the coating: 4.6 cm with the initial height of 1 cm. The value $\eta_m = 468$ Pa $\times$ s corresponds to such an increase in coating height.

The calculation results are shown in Figures 5–7. In Figure 5(a,b), the calculations for the thermocouples fastened at different heights (h_i, experiment; h_i', theory) from the substrate and dependence upon time of the change of the coating height are given as follows:

$$L(t) = \int_0^{L_0} E(\xi, t)\, d\xi$$

The theoretical dependencies are depicted as points to show how a time step was being varied in the computations.

At the initial moment, the thermocouples, which are above the coating, show the flame temperature (1150°C). The algorithm computes temperature only inside the coating; that is, the theoretical temperature–time dependence for above thermocouples contains a discontinuity between the flame temperature and a temperature on a surface of the coating. We showed these discontinuities by using rectangular fragments on the theoretical dependencies [see the dotted lines in Fig. 5(a)]. The experimental indications of these thermocouples are continuous functions on account of thermocouples' relaxation and a temperature gradient within the flame. As foaming proceeds, the thermocouples penetrate into the depth of the material and, naturally, first the temperature decrease is registered. When the velocity of movement of the material of the coating with respect to the thermocouple position significantly decreases, the thermocouple registers the temperature increase. So, if the Euler coordinate is higher than the initial height of the coating, the corresponding temperature–time dependence passes through a minimum.

The temperature change in the points located at the initial moment inside the coating depends on the position of the point and character of foam formation. Usually a preliminary heating of material precedes intensive foaming. That is why one may expect that the temperature in the points situated near the coating surface at small time should increase to a maximum. Then, when an intensive foam formation begins to occur in the coating, the temperature in these points is decreasing. The form of the calculated temperature–time dependence [see curve with $h_i' = 0.8$ cm in Fig. 5(a)] for a thermocouple situated near the surface is probably typical.

Thermocouples located in the lower layers of the coating in the majority of cases show monotonous growth of the temperature [see experimental curve with $h_i = 0$ cm in Fig. 5(a)]. However, in the calculations, the temperature of the substrate passes through the maximum. This maximum is connected with the effect of heat dissipation on the back wall into the external media (a room). In case of the adiabatic back wall ($\alpha_B = 0$), the temperature change should be monotonous, of course.

The model describes the stationary temperature distribution with an appreciable inaccuracy (see Fig. 6). It can be partially explained by the imperfections of eq. (21). It is more probable, however, that the observed discrepancies of the model with experiment are due to the fact that the coating is not actually one-dimensional.

We have noted that, in contrast to the previous models,[1,2,5,6] our model implies an uneven distribution of the final density of the intumescent coating by the depth of the material. The calculated distribution of the final values $E_f(x(\xi))$ of the coating expansion coefficient is shown in Figure 7. It is seen that E_f increases monotonously from the coating surface to the substrate. The upper layers of the coating (~ 0.3 cm) are not foamed at all, for

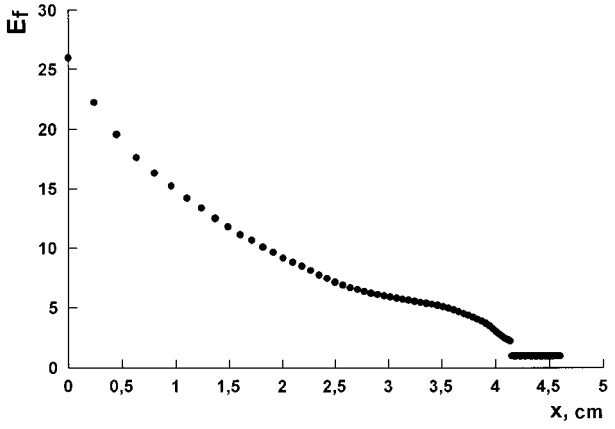

Figure 7 The calculated final distribution of expansion coefficient along a depth of the coating.

carbonization suppresses foaming in accordance with our assumptions.

Generally, the model corresponds to the experiment rather qualitatively than quantitatively. Intensive foam formation in experiment is observed earlier than it follows from the calculations [see Fig. 5(b)]. The assumption abut the legible region $[\eta_m, \infty)$ within which the foam formation takes place, is crude enough. According to this assumption in the temperature range, where viscosity monotonously increases with time, the foam formation either does not occur at all ($\eta < \eta_m$) or occurs irreversibly ($\eta_m < \eta < \infty$). In other words, if the foam formation took place, under the condition $\eta_m < \eta < \infty$ the foam did not settle. It would be more reasonable, however, to suppose that the foam is able to both formation and disintegration at any viscosity, although the rate of its disintegration should decrease with viscosity increasing.

The shortcomings of the model become more intelligible, if considering the space image of a coating [see Fig. 8(a)]. According to the accepted assumptions, the gas released in the layers of a coating, which are located within the zone $0 < x < x\ (\eta_m)$, is not kept in the foam. At the same time, a substance in the lower layers of the coating is liquid, and so the foam in these layers should be hermetic. Thus, more correctly to assume that there exists only one frontier $x=x(\eta \to \infty)$ separating the region of foam formation (a liquid foam) from the region of a porous solid material (a solid foam). However, one may expect that both the models will give close results if the region of the intensive foam formation is rather narrow, actually, if it is commensurable with a size of a bubble. Note that there are known compositions with very sharp transition from viscoelastic state into solid state, for example, the well-known composition called[11] "pharaoh's snake." The considered model seems to reflect the properties of such systems quite satisfactorily. However, we shall consider the other model too.

Model of Foam Draining

Creation of a strict theory of formation and growth of foams is a separate and very complicated problem. To our knowledge, it is unsolved up until now. Nevertheless, let us attempt to develop a simplest model of the foam formation dy-

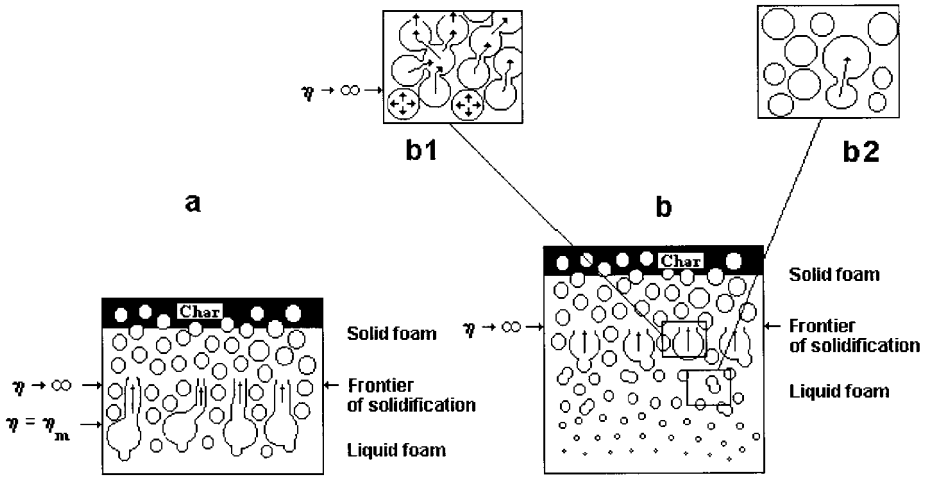

Figure 8 Two models of the foam formation: (a) the model implying the lower critical limit of viscosity η_m, and (b) the model of foam draining.

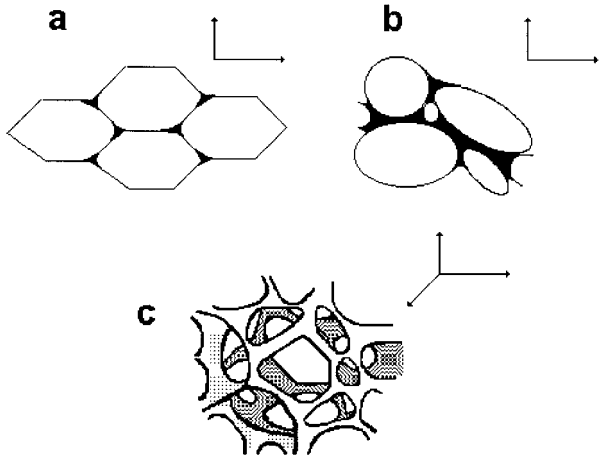

Figure 9 The structures providing for the high gas-filling of a foam: (a) the honeycomb structure, (b) spherelike bubbles of different sizes, and (c) the reticulated structure.

namics by using some phenomenological assumptions.

In contrast to porous materials, a liquid foam hinders a passage of a gas through itself. Each bubble is surrounded by its neighbors [see Fig. 8(b2)]. If a bubble is situated in a depth of a liquid foam, the gas from that bubble can be transmitted only into an adjacent bubble, but it cannot pass directly into atmosphere. Consequently, the gas flow through a foam should be connected exclusively with the process of gas redistribution between bubbles. Only bubbles in the last layer of the liquid foam, being situated on the boundary with the porous solid material, are able to transmit gas directly into atmosphere [see Fig. 8(b1)].

It is worthwhile to note that the images of bubbles in the form of spheres (see Fig. 1–3 and 8) are, of course, only schematical. If all bubbles had the ideal spherical form and an identical size, the maximal quota of gas in the foam would constitute $\omega_g = 0.7405$ (or $E = 3.85$). An observable factor of foaming frequently exceeds the value of 3.85; for example, in a number of cases, it reaches a value $\sim$ 100. The variants of cellular structures[12] shown in Figure 9 allow one to explain high values of ω_g (or E).

We suppose in the region of the liquid foam, only hermetic (closed) hollows can arise [see Fig. 9 (a,b)]. Numerous research on microscopic sections of the coatings show[13] that the form of hollows is actually more complicated than that represented in Figure 9. We find it hard to give any statistics; we can only note that some combination of honeycomb structure [see Fig. 9(a)] and ball-like bubbles [see Fig. 9(b)] is observed in reality.

As to reticulated structure [see Fig. 9(c)], it is formed in the region of solid foam as result of destruction of bubbles walls, owing to high gas pressure or exhausting the material of the walls because of chemical pyrolysis. The reticulated structure, as well as the closed porous structure, does not possess regular geometry. It is some cellular space pierced by a great number of chaotically located microscopic channels and cracks.

The solid foam is a "frozen" formation; therefore, to describe an intumescence, one should consider the region of the liquid foam.

Let us consider a layer between two characteristics, $x_1(\xi_1,t)$ and $x_2(\xi_2,t)$. When foaming, a mass of polymeric substance within this layer is conserved. As to accumulation of gas in this layer, it depends upon a difference between gas flow, which leaves the layer towards the surface of the coating, and a flow coming to the layer under consideration from lower layers. If a thickness of a chosen layer of the foam is commensurable with a size of a bubble, the flow going out from this layer should depend only upon properties of the foam inside the layer and it should not depend upon a properties of lower layers. In particular, an outlet of gas into atmosphere is determined by properties of the foam interface between solid and liquid foams.

Stability of foams is determined by thermodynamic and kinetic factors. As known, the thermodynamic stability is reached by means of introduction of detergents into a liquid. It is worthwhile to note that all attempts[13] to use detergents to rise effectiveness of intumescence of polymer compositions did not lead to appreciable successes. In the case of polymer foams, the kinetic factor, that is, a totality of relaxation processes connected with a movement of a liquid in walls of bubbles, is likely to prevail. This movement, in turn, is controlled by viscosity of a material. It is reasonable to assume that, other things being equal, the rate of disintegration of bubbles is inversely proportional to viscosity.

The more the amount of gas per unit of a foam volume, the thinner the walls of bubbles and, consequently, the greater the probability of rupture of bubbles and transmission of gas into adjacent bubbles (or into atmosphere).

Let us consider a layer of bubbles at the distance $x = x_2$ from substrate. Taking account of the suppositions mentioned above, the gas flow to-

wards the surface of the coating may be written as

$$\rho_g v_{g|x=x_2} = k_d[(E - 1 + q)/\eta]_{|x=x_2} \quad (32)$$

where k_d is some empirical parameter (the parameter of the foam draining) value of which will be considered as being a constant for all layers of the liquid foam.

Let L_b^E be a characteristic (effective) size of a bubble in the Euler coordinate. As a result of destruction of bubbles in the layer located at the distance $x = x_1 \cong x_2 - L_b^E$, the amount of gas, which comes per unit of time into the layer under consideration, is equal to

$$\rho_g v_{g|x=x_1} = k_d[(E - 1 + q)/\eta]_{|x=x_1} \quad (33)$$

This gas is retained by the layer of the foam and is expended in a formation of new bubbles. Let us assume that the height of the foam considerably exceeds the size of bubbles. In other words, one can use the limit $L_b^E \to 0$. Then, replacing the flows in eq. (15) by expressions (32) and (33) instead of eq. (17), we obtain

$$\partial/\partial t[E - 1 + q)\rho_g] + \partial/\partial\xi[k_d(E - 1 + q)/\eta] = \rho_0 dq/dt \quad (34)$$

An initial condition has the form

$$E(\xi, 0) = 1,\ q(\xi, 0) = 0 \quad (35)$$

Since equality [eq. (17)] turns into a partial equation [eq. (34)] for determination of E, we replaced in eq. (17) the full derivative with respect to time by partial derivative.

A boundary condition on the back wall is needed for closure of the system of equations. Note that when deducing this condition, in contrast to deducing eq. (34), one cannot use the limit $L_b^E \to 0$.

With increasing a quota of gas in the foam, the effective L_b^E size must increase. This size is connected with the expansion coefficient by a complex manner. However, we shall use the simplest approximation, as follows: $L_b^E = E\,L_b^L$, where L_b^L is a minimum characteristic size of a bubble. Inasmuch as $(x_2 - x_1)/(\xi_2 - \xi_1) \approx \partial x/\partial\xi = E = L_b^E/L_b^L$, and consequently, $L_b^L = \xi_2 - \xi_1$, the L_b^L value can be called a characteristic size of a bubble in Lagrange coordinate.

The condition of impermeability of the substrate has the form $\rho_g v_{g\,|\,\xi=0} = 0$. At the same time, in the region $\xi > 0$, the functions E, q, and η are continuous ones; therefore, from eq. (34), we have

$$\lim_{\delta\to 0} (\rho_g v_{g|\xi=0+\delta} - \rho_g v_{g|\xi=0})/\delta = \infty$$

Thus, the flow on the back wall contains a discontinuity. After integration of eq. (34) from 0 to L_b^L, when assuming $\rho_g v_{g|\xi=0+0} = \rho_g v_{g|\xi=L_b^L}$, we obtain

$$d/dt[(E - 1 + q)\rho_g]_{|\xi=0+0} - \rho_0 dq_{|\xi=0+0}/dt = -\{[k_d(E - 1 + q)/\eta]_{|\xi=0+0}\}/L_b^L \quad (36)$$

The integration along Lagrange coordinate from $\xi_1 = 0$ to $\xi_2 = L_b^L$ is equivalent to integration along Euler coordinate from $x_1 = 0$ to $x_2 = E\xi_2 = EL_b^L = L_b^E$. Thus, the assumption $L_b^E = EL_b^L$ conforms to the condition of mass conservation in the lowest layer of the coating.

The left-hand part of eq. (36) is, certainly, a finite function; that is why eq. (36) allows the transition $L_b^L \to 0$ only if $E(0 + 0,t) - 1 + q(0 + 0,t) = 0$. However, the functions $E(0 + 0,t)$ and $q(0 + 0,t)$, according to the physical sense, can vary with time. Thus, by using the rule of contraries, one may conclude that the model implies only finite values of L_b^L (and L_b^E). Indeed, if a height of a foam is commensurable with a size of a bubble, the speculative breaking up of the foam into layers loses a physical sense.

Let us consider how the draining of the foam evolves in the simplest situation; when in all layers the parameters η and ρ_g are constant, there are no interior sources of gas in the foam ($dq/dt = 0$), and, initially, the foam is filled evenly ($E(\xi,0) = E_0$).

It is convenient to introduce the following dimensionless parameter: $B = \eta\rho_g L_f/(\tau_b k_d) = L_f/L_b^L$, where $\tau_b = \eta\rho_g L_b^E/\mathrm{k_d}$ is the characteristic time of life of a bubble, and L_f is a final height of the liquid after complete settling of the foam. Now eq. (34), together with boundary and initial conditions, may be rewritten as

$$B\partial E/\partial(t/\tau_b) = \partial E/\partial(\xi/L_f) \quad (37)$$

$$dE(0 + 0, t)/d(t/\tau_b) = -(E(0 + 0, t) - 1);$$

$$E(\xi, 0) = E_0,\ 0 < \xi < L_f \quad (38)$$

One of the easy methods of solving the system of eqs. (37) and (38) consists in using the Laplace transformation, which links any pre-image $Z(t)$ with its functional image $\hat{Z}(s)$ by means of the following integral equation:

$$\hat{Z}(s) = \int_0^\infty Z(t)\exp(-st)dt$$

where s is the parameter of the transformation. One may readily deduce expressions for the Laplace transforms of the functions $L(t)$ and $E(\xi,t)$. These are

$$\hat{E}(\xi, s) = E_0/s - (E_0 - 1)\exp(-s\xi\tau_b B/L_f)/[s(s\tau_b + 1)]$$

$$\hat{L}(s) = E_0 L_f/s - (E_0 - 1)(L_f/\tau_b B) \times [1 - \exp(-s\tau_b B)]/[s^2(s\tau_b + 1)]$$

Making use the tables of inversion of Laplace transforms[14,15] and applying some theorems,[15] in particular, the delay theorem, we obtain

$$(E(\xi, t) - 1)/(E_0 - 1) = \begin{cases} 1, & t/\tau_b < \xi B/L_f \\ \exp(\xi B/L_f - t/\tau_b), & t/\tau_b > \xi B/L_f \end{cases} \quad (39)$$

$$(L(t)/L_f - 1)/(E_0 - 1) = \begin{cases} 1 - B^{-1}[t/\tau_b - 1 + \exp(-t/\tau_b)], & t/\tau_b < B \\ B^{-1}\exp(-t/\tau_b[\exp(B) - 1], & t/\tau_b > B \end{cases} \quad (40)$$

The functions expressed by eqs. (39) and (40) are represented in Figures 10 and 11. The character of distribution of gas in the foam depends upon the ratio of height of the foam to the effective size of a bubble. With the large parameter B, the profile $E(\xi,t)$ looks like a step function [see Fig. 10(a)]. This means an occurrence of the legible mobile frontier ($\xi^* = tL_b^L/\tau_b$) in the foam that separates a liquid with a low content of gas ($0 < \xi < \xi^*$) from the gas-filled part of the foam ($\xi^* < \xi < L_f$). In the course of draining the foam, the height of the liquid is increasing, while the height

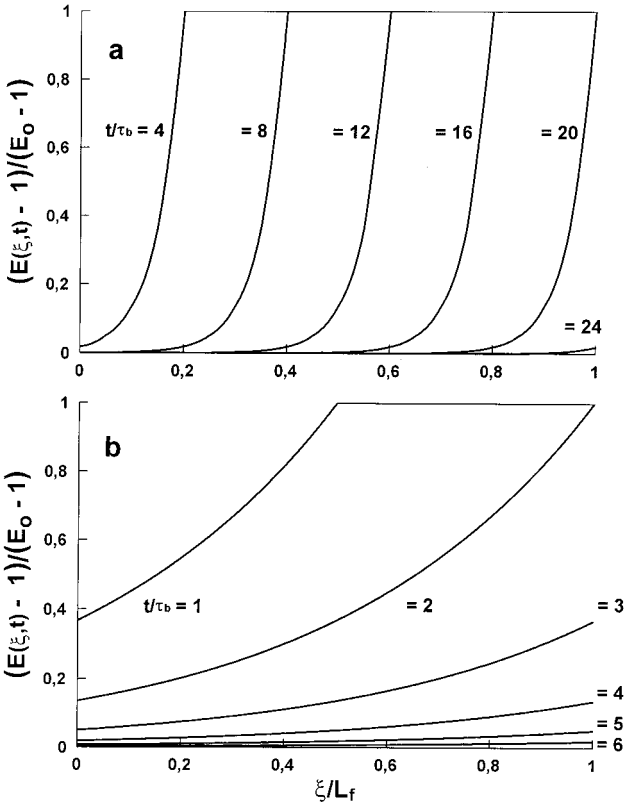

Figure 10 The profiles of the expansion coefficient corresponding to different values of the parameter B and different moments of the reduced time, t/τ_b: (a) $B = 20$; (b) $B = 2$.

of the gas-filled part is decreasing. The constancy of the expansion coefficient within the region $\xi^* < \xi < L_f$ does not mean an absence of a gas flow in this part of the foam. Merely, an amount of gas that comes into each chosen layer of the foam from lower layers is equal to an amount of gas that leaves the given layer because of disintegration of bubbles.

The step distribution of the density leads to a constancy of the foam settling. Indeed, it follows from eq. (40) that with the parameter $B >> 1$ (see Fig. 11, curve 2), the decrease of the foam height with time occurs almost linearly, as follows:

$$(L(t)/L_f - 1)/(E_0 - 1) = (B - t/\tau_b)/B \quad (41)$$

If a height of the foam is commensurable with a size of a bubble ($B \cong 1$), the foam is being destroyed almost evenly along its depth. In the latter case, eq. (41) gives a bad accuracy (see Fig. 11, curve 1).

With an even distribution of gas within the foam, the extension coefficient ceases to depend

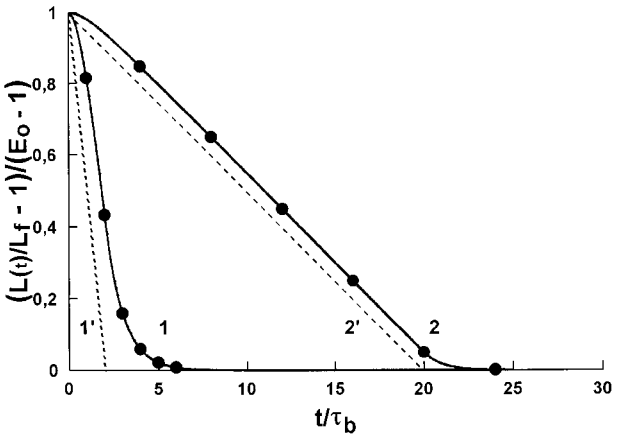

Figure 11 The dependence of the reduced height of a foam upon the reduced time with the different parameters B: 1–2, and 2–20. Linear dotted lines (1′, 2′) correspond to eq. (41). The points correspond to the time moments in Figure 10.

upon a coordinate; that is $E(\xi,t) = E(t)$. If $B \to 0$, from eqs. (39) and (40), we have

$$(E(t) - 1)/(E_0 - 1) = \exp(-t/\tau_b) \qquad (42)$$

$$(L(t)/L_f - 1)/(E_0 - 1) = \exp(-t/\tau_b) \qquad (43)$$

In this case, the time of life of a bubble limits the time of life of the foam as a whole.

Although in the situation $B \cong 1$ ($L_f \cong L_b^L$), as mentioned above, the model in many respects loses a physical sense, but eqs. (42) and (43) remain phenomenologically correct. From here, one may conclude that the use of the characteristic time τ_b from phenomenological standpoint is more preferable in comparison to the characteristic size L_b^L. The latter appears in eq. (36), which can be rewritten, however, as follows:

$$d/dt[(E - 1 + q)\rho_g]_{|\xi=0+0} - \rho_0 dq_{|\xi=0+0}/dt = -\rho_g[(E - 1 + q)/\tau_b]_{|\xi=0+0}$$

The presence of ρ_g in the expression $\tau_b = \eta\rho_g L_b^L/k_d$ seems strange. As the drain of the foam should not depend upon ρ_g, we should use $k_d^*\rho_g$ instead of k_d, and then $\tau_b = \eta L_b^L/k_d^*$. If substituting $k_d = k_d^*\rho_g$ in eqs. (32) and (33), the new constant k_d^* determines a linear velocity of gas and not the mass flow. Therefore, the use of k_d^* is more correct. At the same time, the density ρ_g varies rather weakly and can be considered as a constant. That is why both the approaches are almost equivalent.

The model considered implies a reversibility of intumescence. According to eq. (34), the foam settles if gas formation ceases. The foam can retain a constant height if expansion of the foam, resulting from formation of new bubbles owing to interior sources of gas, compensates the foam settling because of the disintegration of bubbles. These peculiarities of the model are adequate to reality. At the same time, the model contains a number of appreciable shortcomings. A principal defect is that it does not take into account a size distribution of bubbles, while this distribution must considerably influence the foam stability. Besides, in the case of intumescent coatings, it is vague to what extent the stability and other properties of the foam may be affected by capillary and surface effects arising on the interface between liquid and solid foams. In spite of above-mentioned imperfections, the considered model seems very useful at the given stage of the theory development.

The heat transfer equation [eq. (20)] and eq. (34), together with initial and boundary conditions given by eq. (22), (23), (24), (35), and (36), are the complete system for computing all properties of a coating. For solving the system, we used a finite difference method being similar to the algorithm considered in the previous section.

An integration of eq. (34) was carried out by the explicit Euler method. To achieve good accuracy, it is necessary to use a very small time step. It was diminished, as the viscosity, calculated at some knot of the space grid, increased to infinity ($\eta \to \infty$). Then a time step first was increased and then was being diminished again, as the viscosity at the next knot grew. Because of a discreteness of the space grid, the function $L(t)$ in the computations looks like a step function, and the temperature, being calculated in the Euler coordinate system as a function of time, for the same reason slightly oscillates. In Fig. 12, only points corresponding to fulfilling the condition $\eta \to \infty$ at knots of the grid are shown. That is why the high-frequency oscillations are not observed on these curves.

A study of slits of the coating shows that the size of bubbles $L_b^E \sim 0.1$ cm is typical for foamed layers. With the expansion coefficient ~ 5, we have $L_b^L = L_b^E/E = 0.02$ cm. The latter value was taken for the calculations.

In order to complete a choice of parameters, one should find one more constant, namely, k_d/η_0, where η_0 is the constant in the Arrhenius equa-

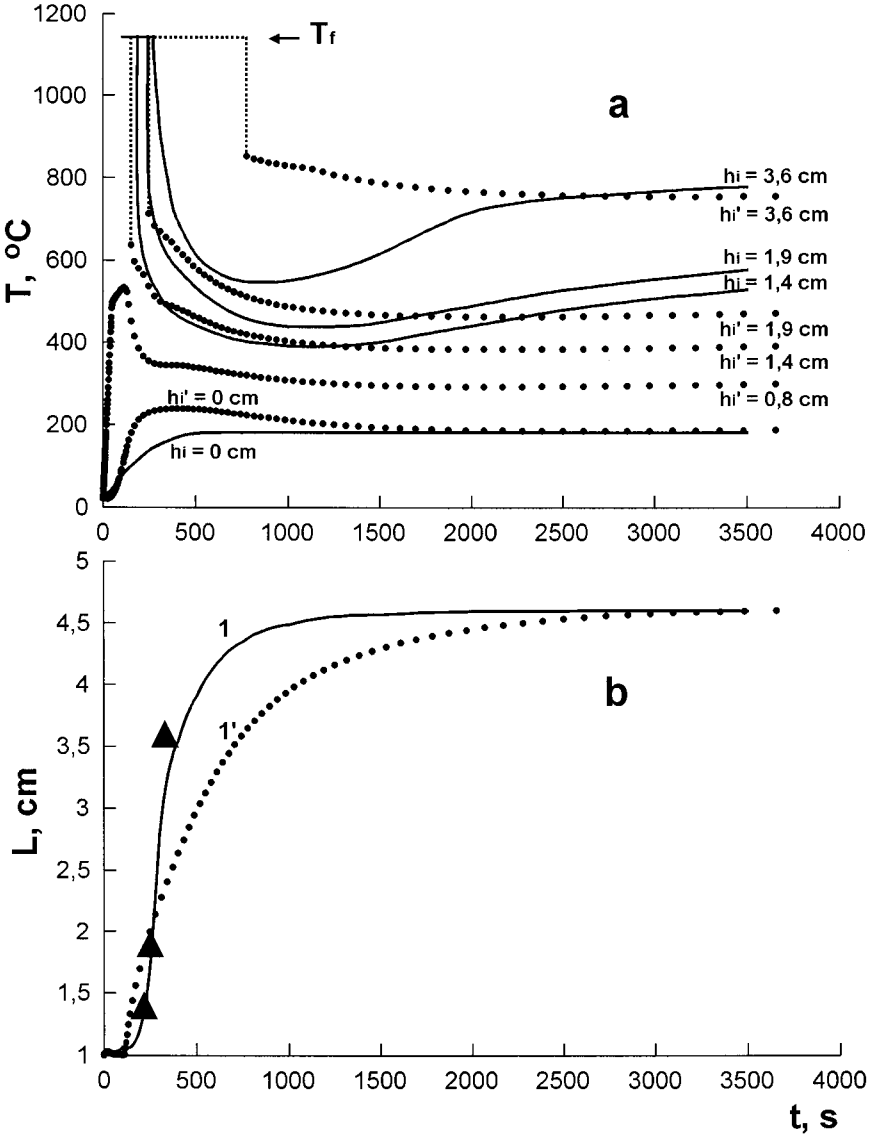

Figure 12 The same as in Figure 5 but for the model of foam draining.

tion for viscosity.[3] The value of $k_d/\eta_0 = 3.6 \times 10^2$ g/s $\times$ cm^2 was chosen so that the final height of the coating in the calculations would correspond to the experiment (4.6 cm).

The constant $\eta_0 = 2.4 \times 10^{-4}$ Pa $\times$ s has been estimated earlier.[3] With $M = 30$ g at 300°C, the gas density ρ_g is equal to 6.4×10^{-4} g/cm^3. Thus, we are able to estimate the lifetime of bubbles $\tau_b = \eta\rho_g L_b^L/k_d$. At the viscosity 3000 Pa $\times$ s, the value of $\tau_b = 0.44$ s corresponds to the parameters obtained.

In Figures 6, 12, and 13 are shown the dependencies computed for the model of the foam draining. By comparing them with those represented above for the model implying the lower critical threshold of viscosity, one may conclude that both the models give close results when calculating the temperature field, the change of the coating height with time, and the stationary temperature profile. However, results of the computation of a stationary density distribution differ qualitatively (compare Fig. 7 with 13).

The first model predicts that lower layers of coating are to foam most effectively, while according to the second one, the lower layers do not practically foam. A study of slits of the coating after foaming shows that for the considered composition the distribution with maximum of the expansion coefficient (see Fig. 13) corresponds better to the experiment. Namely, the lowest lay-

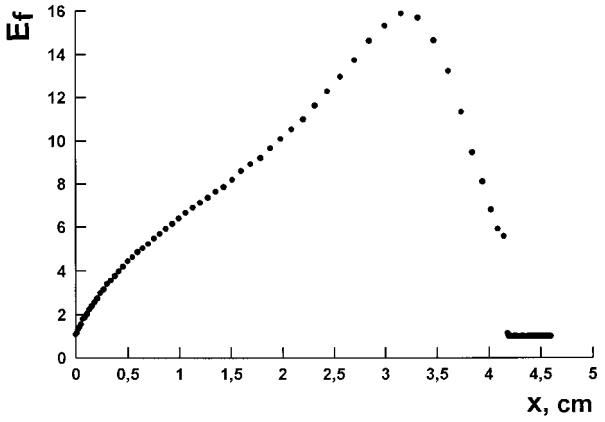

Figure 13 The same as in Figure 7 but for the model of foam draining.

ers of the coating are less gas-filled than central ones. However, to argue convincingly the used assumptions, additional experimental and theoretical researches are required.

CONCLUSIONS

A new algorithm is proposed for predicting fireproof properties of the intumescent materials by using their characteristics measured in independent experiments. Two models of foam formation were studied within the general thermophysical problem. Both the modes lead to close results when calculating a temperature field in a coating. Thus, a temperature field itself cannot serve as a measure of adequacy of a model.

The temperature profiles computed differ considerably from experimental ones. The accepted assumption that the coating is flat apparently stipulates this discrepancy with the experiment. It is quite obvious, in those experiments where a size of a substrate is commensurable with a height of a swollen material, the coating cannot be considered in one-dimensional approximation, for the boundary effects on a perimeter of the coating in this case can considerably influence the process of foam formation.

In contrast to preceding algorithms, the offered one takes into account changing the rheological properties controlled by kinetics of curing the material. The necessary constants can be found from isotherms of viscosity. On the other hand, the increase of viscosity determines stability of the foam. Therefore, the considered approach gives an idea as to how one may govern the foam formation and, consequently, the useful properties of the coatings by means of modifying chemical parameters of the system.

For a further improvement of the model and a confirmation of correctness of the accepted assumptions, a more detailed study of the mechanism of the foam formation in polymer systems is needed.

The work was fulfilled partially with the financial support of INTAS, project INTAS–93–1846.

REFERENCES

1. D. E. Cagliostro, S. R. Riccitiello, K. J. Clark, and A. B. Shimizu, *J. Fire & Flammability,* **6,** 205 (1975).
2. C. E. Anderson and D. K. Wauters, *Int. J. Eng. Sci.,* **22,** 881 (1984).
3. V. Sh. Mamleev and K. M. Gibov, *J. Appl. Polym. Sci.,* **66,** 319 (1997).
4. K. M. Gibov and V. Sh. Mamleev, *J. Appl. Polym. Sci.,* **66,** 329 (1997).
5. J. Buckmaster, C. E. Anderson, and A. Nachman, *Int. J. Eng. Sci.,* **24,** 263 (1986).
6. C. E. Anderson, J. J. Dziuk, W. A. Mallow, and J. Buckmaster, *J. Fire Sci.,* **3,** 161 (1985).
7. Ya. B. Zeldovich and A. D. Myshkis, *Elements of Mathematical Physics: A Medium of Noninteracting Particles,* Nauka, Moskow, 1973 (in Russian).
8. C. E. Anderson, J. D. E. Ketchum, and W. P. Mountain, *J. Fire Sci.,* **6,** 390 (1988).
9. A. V. Likov, *Theory of Heat Conduction,* Visshaya shkola, Moscow, 1967 (in Russian).
10. A. A. Samarski, *Theory of Difference Schemes,* Nauka, Moscow, 1977 (in Russian).
11. H. Remy, *Lenrbuch der Anorganischen Chemie,* Vol. 2, Verlagsgellshaft Geest, Portig K.-G., Leipzig, 1961.
12. A. A. Berlin and F. A. Shutov, *Chemistry and Technology of Gas-Filled High-Polymers,* Nauka, Moscow, 1980 (in Russian).
13. K. M. Gibov, *Fire-Proof Intumescent Coatings for Woody and Metallic Constructions; Final Report O-AH-77, 01.84.0056141,* All-Union Institute of Scientific and Technical Information, Moscow, 1985 (in Russian).
14. G. A. Korn and T. M. Korn, *Mathematical Handbook for Scientists and Engineers,* McGraw-Hill, New York, 1968.
15. G. Doetsch, *Anleitung zum pructischen gebrauch der Laplace–transformation und der z-transformation,* Birkhäuser Verlag, München, 1967.